Continuous Indoor Tracking via Differential RSS Fingerprinting

Yunzhi Li*, Yidan Hu†, Aishah Aseeri‡, Yukun Dong*, and Rui Zhang*
*Department of Computer and Information Sciences, University of Delaware, Newark, DE 19716
† Department of Computing Security, Rochester Institute of Technology, Rochester, NY 14623
‡Department of Information Technology, King Abdulaziz University, Jeddah 22254, Saudi Arabia
{liyunzhi,yukun,ruizhang}@udel.edu, yidan.hu@rit.edu, aaaseeri@kau.edu.sa

2022 IEEE 19th International Conference on Mobile Ad Hoc and Smart Systems (MASS) | 978-1-6654-7180-0/22/$31.00 ©2022 IEEE | DOI: 10.1109/MASS56207.2022.00072

***Abstract*—Indoor navigation is necessary for users to explore large unfamiliar indoor environments such as airports, shopping malls, and hospital complex, which relies on the capability of continuously tracking a user's location. A typical indoor navigation system is built on top of a suitable Indoor Positioning System (IPS) and requires the user to periodically submit location queries to learn their whereabouts whereby to provide update-to-date navigation information. Received signal strength (RSS)-based IPSes are considered as one of the most classical IPSes, which locates a user by comparing the user's RSS measurement with the fingerprints collected at different locations in advance. Despite its significant advantages, existing RSS-IPSes suffer from two key challenges, the ambiguity of RSS fingerprints and device diversity, that may greatly reduce its positioning accuracy. In this paper, we introduce the design and evaluation of CITS, a novel RSS-based continuous indoor tracking system that can effectively cope with fingerprint ambiguity and device diversity via differential RSS fingerprint matching. Detailed experiment studies confirm the significant advantages of CITS over prior RSS-based solutions.**

I. Introduction

Indoor navigation is necessary for users to locate themselves and reach their destinations in large unfamiliar venues such as airports, shopping malls, and hospital complex, where GPS signals are either absent or unavailable. According to a recent report [1], the global market of indoor positioning and navigation service is expected to reach 256.59 billion in 2028.

The capability of continuously tracking a user's locations is key to any indoor navigation system, which is required for computing and updating the optimal route from the user's current location to intended destinations and providing the user with visual or audio turn-by-turn instructions. As a result, a typical indoor navigation system involves an Indoor Positioning System (IPS) module and requires the user to periodically submit location queries to learn their whereabouts. Existing indoor navigation systems mainly differ in the technology behind their IPS modules, which include Computer Vision [2]–[4], RFID [5]–[7], Wi-Fi [8] [9], visible light [10]–[12], Bluetooth [13]–[15], acoustic sound [16] [17] and so on.

WiFi Received Signal Strength-based IPS (RSS-IPS) [8] [9] is considered as one of the most classical IPSes, which exploit distinguishable RSSes at different locations as their fingerprints and locates a user by comparing the user's RSS measurement with the RSS fingerprints collected at different locations in advance. In comparison with other types of IPSes, RSS-based IPSes explore ubiquitous smartphones and WiFi infrastructure widely available in target venues and do not require costly infrastructure updates. A typical RSS-IPS works in two phases. In the offline training phase, the IPS operator collects RSS fingerprints at different indoor reference locations. In the online positioning phase, on receiving an RSS measurement from a user, the IPS server returns the reference location of which the RSS fingerprint is the closest to the user's measurement.

RSS-IPSes face two critical challenges that limit their positioning accuracy in practice, the ambiguity of RSS fingerprints and device diversity. First, prior studies such as [18] [19] have shown that multiple locations could have the same RSS fingerprint. As a result, it is difficult for the IPS server to distinguish these locations solely based on the user's RSS measurement. Second, it is also well known that different mobile devices may detect different Received Signal Strengths at the same location and time [20]–[23]. In particular, the device used by the IPS operator to collect the RSS fingerprints may be different from the mobile devices used by the users during the online navigation phase, which means that the RSS measurement collected by the user may be different from the RSS fingerprint at the location. Both factors could result in larger differences between the RSS fingerprint and the user's RSS measurement at the same location and reduce the positioning accuracy achieved by RSS-IPSes.

Fortunately, we find that periodic location queries from the user during indoor navigation offers new opportunities to tackle WiFi fingerprint ambiguity and device heterogeneity. Specifically, instead of matching a user's RSS measurement with the fingerprint, we find that matching the difference between adjacent RSS measurements with the difference between RSS fingerprints at adjacent locations offers great resilience to device diversity. Moreover, the ambiguity of WiFi fingerprints can be effectively tackled by matching a sequence of RSS measurements from user to a movement path. Based on these observations, we introduce the design and evaluation of CITS, a novel continuous RSS-based indoor tracking system that can achieve high positioning accuracy in the presence of WiFi fingerprint ambiguity and device heterogeneity. Our contributions in this paper are summarized as follows.

- We are the first to study continous indoor tracking in the

2155-6814/22/$31.00 ©2022 IEEE
DOI 10.1109/MASS56207.2022.00072

presence of fingerprint ambiguity and device diversity.
- We introduce CITS, a novel RSS-based IPS based on differential fingerprinting and path matching that can achieve much improved positioning accuracy.
- Experiment studies based on a prototype confirm the advantages of CITS over prior RSS-based IPSes. For example, our experiment results show that CITS achieves a mean distance error at 0.8 m in contrast to the 1.68 m reported in [8] when the user travels more than 25 seconds in the indoor environment.

The rest of this paper is structured as follows. Section II discusses the related work. Section III presents the design of CITS. Section IV reports our experiment results. This paper is finally concluded in Section V.

II. Related Work

In this section, we review some of the prior works that are most germane to our work.

A conventional technique for indoor tracking is the pedestrian dead reckoning (PDR) [24]. A PDR system records the Inertial Measurement Unit sensor readings when the user is moving and calculates the user's displacements to determine his current location. Since the displacement error accumulates with the user's moving, several types of indoor signals have been explored to augment the PDR. Fang *et al.* [25] enhanced the PDR system with wireless telemetry. Carrera *et al.* [26] fused RSS, PDR, and building information to track the user's movement. In [27], Samuel *et al.* corrected the error of PDR systems in a smart building environment. They equipped the user with a RFID tag reader to read the RFID tags which are placed throughout the smart building then correct the cumulative error by reading the tags. Recently, hybrid algorithms have been proposed in [28]–[30] to highly improve the positioning accuracy via combining PDR approach with WiFi fingerprinting approach. Shen *et al.* [31] pointed out that user's heading error is the key factor of the error in PDR, and used WiFi-RSS to minimize the heading error resulting in a higher position accuracy in PDR. In [32], Ho *et al.* removed the interference signals for interior sensor reading with a fast Fourier transform-based smoother on the collected data then further improved the PDR accuracy. In addition, exploring the magnetic field information is another promising way to minimize the accumulating error in PDR [33]–[35]. Apart from the above papers, there still exist plenty of works that involve PDR. However, none of them consider the heterogeneous device problem. In other words, the heterogeneous device problem impacts the process of correcting the accumulating error.

Apart from PDR, researchers also try to track the user with WiFi signals. Yang *et al.* [36] analyzed the localization errors of the RSS-based fingerprinting localization methods. Hoang *et al.* [37] inputted a series of WiFI RSS into hidden Markov chain (HMM) to predict the user's movement. In [38], Anthea *et al.* proposed a novel RSS indoor tracking system by using a Compressive Sensing-based positioning scheme. Channel station information has been used to infer the user's movement and activity in [39], [40]. Kleisouris *et al.* [41] utlized multiple antennas to improve localization results, while Zheng *et al.* [42] combined multiple frequencies and powers to reduce the localization errors. A RSS gradient fingerprint database was constructed in [43] to track user's movement with improved accuracy via comparing the RSS gradient between each two locations. Liu *et al.* [44] combined acoustic ranging and RSS-based localization to reduce the large errors of smartphone tracking. In [45], Yang *et al.* proposed a improved lateration based method for mitigating multipath effects. Hernndez *et al.* [46] used a topological RSS radio-map then tracked the user's location through Bayes filter. Chandrasekaran *et al.* [47] compared the performance of several widely used RSS based localization algorithms under a laboratory setting. Recently, Mai *et al.* [48] utilized convolutional neural network (CNN) and Tiwary *et al.* [49] trained a deep neural network based on RSS difference to track the users in the indoor environment. There are some research efforts dedicated to robust indoor localization, such as robust localization in the presence of signal strength and access point attacks in [50]–[52]. However, the above works do not consider the heterogeneous problem or solve this problem under a very strict condition with a strong assumption.

Besides WiFi signals, there are also several other types of IPSes based on other different technologies. For example, image-based IPSes have been proposed in [2]–[4] to locate users with high positioning accuracy through recognizing landmarks in the photos. Apart from image-based IPSes, acoustic signal-based IPSes [16], [17] utilized acoustic signals as fingerprints for localization. In addition, visible light [10]–[12], Radio Frequency Identification (RFID) [5]–[7], and Bluetooth signals [13]–[15] could also been used for user positioning. However, the above works can only repetitively infer the user's location in a tracking system instead of considering user's prior locations.

III. CITS Design

In this section, we first give an overview and then detail CITS's design.

A. Overview

We design CITS based on two key ideas.

First, we observe that matching the difference between two adjacent RSS measurements from the user to the difference between two RSS fingerprints can effectively mitigate the impact of device diversity. Specifically, several prior studies [20]–[23] have shown that for any two different devices, say A and B, there is a linear relationship between their RSS measurements from the same AP at the same location and time. In particular, let rss_A and rss_B be the RSS measurements of devices A and B, respectively. We have

$$\mathsf{rss}_A = \theta \cdot \mathsf{rss}_B + \delta_{AB} \ , \tag{1}$$

where θ and δ_{AB} are two device-dependent constants. Moreover, it has also been shown in [23] that the parameter θ is close to one in most cases, which is also used in recent work

example.png

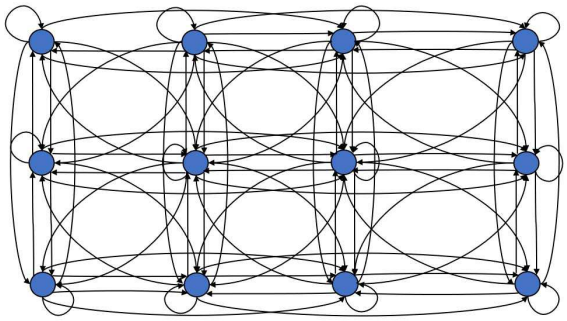

Fig. 1. An example of the graph with 12 vertexes, i.e., reference locations.

[53]. This allows us to ignore parameter θ hereafter and rewrite Eq. (1) as

$$\mathsf{rss}_A = \mathsf{rss}_B + \delta_{AB} \ , \tag{2}$$

Further let rss'_A and rss'_B denote the RSS measurements of the two devices at a different location. We get

$$\mathsf{rss}'_A = \mathsf{rss}'_B + \delta_{AB} \ . \tag{3}$$

Subtracting Eq. (3) from Eq. (2), we have

$$\mathsf{rss}_A - \mathsf{rss}'_A = \mathsf{rss}_B - \mathsf{rss}'_B \ , \tag{4}$$

which indicates that the difference of device A measurements at the two locations is the same as that of device B even if they are of different device models.

Second, we find that the ambiguity of RSS fingerprints can be addressed by path matching that takes a user's prior estimated locations into accounts. In particular, assume that the time is divided into intervals of same length and that a user submits one RSS measurement collected by a mobile device of an unknown type at each time interval $t = 1, 2, \ldots$. If we know that the user is at reference location x at time t and that the maximum distance a user can travel within one time interval is d, then the user must be at one of the reference locations within a distance of d from reference location x, including reference location x itself if the user has not moved. While it is possible for multiple reference locations share the same RSS fingerprint, by limiting the search space for user's location at time $t+1$ can greatly reduce the chance of such ambiguity.

In what follows, we detail the design of CITS, which consists of *differential RSS fingerprint database construction* and *continuous tracking via path matching*.

B. Differential RSS Fingerprint Database Construction

We first divide the whole indoor venue into n cells of equal size, e.g., 0.5×0.5 m^2, and select the center of each cell as one reference location. We then construct a directed graph $G = (V, E)$, where V is the set of n vertexes with each corresponding to one reference location, and E is the set of edges. Two vertexes x and y are connected by a pair of antiparallel edges edge $e(x, y)$ and $e(y, x)$ if the minimal distance between cell x to cell y is no more than d, where d is a system parameter denoting the maximum distance a user can travel between two consecutive RSS measurements. In addition, every vertex $x \in V$ has a self-loop, i.e., an edge that originates from and terminates at x, to account for the cases that the user remain in the same cell between two consecutive RSS measurements. Fig. 1 shows an example of the graph with 12 vertexes, where two vertexes are neighboring vertexes if there is at most one cell between them.

Assume that there are m WiFi APs in the indoor venue. The CITS operator collects one RSS fingerprint $\mathsf{rss}_x = (\mathsf{rss}_x^1, \ldots, \mathsf{rss}_x^m)$ at each reference location $x \in V$, where rss_x^j is the RSS of AP j for all $1 \le j \le m$.

Next, for every edge $e(x, y) \in E$, we calculate the RSS difference between vertexes x and y as

$$\triangle\mathsf{rss}_{x,y} = (\triangle\mathsf{rss}_{x,y}^1, \ldots, \triangle\mathsf{rss}_{x,y}^m) \ . \tag{5}$$

where

$$\triangle\mathsf{rss}_{x,y}^j = \mathsf{rss}_y^j - \mathsf{rss}_x^j \ ,$$

is the difference between the AP j's RSS fingerprints at reference locations x and y for all $1 \le j \le m$.

Finally, we store the constructed RSS differential fingerprint database as $\{\mathsf{rss}_x | x \in V\} \bigcup \{\triangle\mathsf{rss}_{x,y} | e(x, y) \in E\}$.

C. Continuous Tracking via Path Matching

With the differential WiFi fingerprint database in place, we now illustrate how to continuously track a user via path matching. Denote by $\mathsf{rss}_t = (\mathsf{rss}_t^1, \ldots, \mathsf{rss}_t^m)$ the user's RSS measurement at time $t = 1, 2, \ldots$, where rss_t^j is the RSS measurement for AP j for all $1 \le j \le m$. Consider two adjacent RSS measurements rss_{t-1} and rss_t. We define the RSS difference for AP j from time $t-1$ to time t as

$$\triangle\mathsf{rss}_t = (\triangle\mathsf{rss}_t^1, \ldots, \triangle\mathsf{rss}_t^m) \ ,$$

where $\triangle\mathsf{rss}_t^j = \mathsf{rss}_t^j - \mathsf{rss}_{t-1}^j$ for all $1 \le j \le m$.

Now consider an edge $e(x, y) \in E$ with RSS difference $\triangle\mathsf{rss}(x, y)$. Intuitively, if $\triangle\mathsf{rss}_t \approx \triangle\mathsf{rss}(x, y)$, then it is likely that the user has moved from reference location x to y between time $t-1$ and t. Based on this observation, we further define the overall RSS difference with respect to time t and edge $e(x, y)$ as

$$\phi(t, e(x, y)) = \sum_{j=1}^{m} |\triangle\mathsf{rss}_t^j - \triangle\mathsf{rss}_{x,y}^j| \ .$$

Similarly, for any path $p = \langle x_1 \to x_2 \to \cdots \to x_t \rangle$ consisting of a sequence of t vertexes, we define the overall path RSS difference as

$$\phi_p = \sum_{i=2}^{t} \phi(i, e(x_{i-1}, x_i)) \ .$$

The smaller ϕ_p, the more likely the user traverses path p from time 1 to t.

The CITS server always maintains the s most likely paths the user traverses that have the smallest overall path RSS

difference, where $s \geq 1$ is a system parameter. Upon receiving a new RSS measurement rss_t from the user at time t, the CITS server recomputes the s most likely paths. Let $p_\varphi = \langle x_1^\varphi \rightarrow \cdots \rightarrow x_{t-1}^\varphi \rangle$ denote the φth most likely path at time $t-1$ for all $1 \leq \varphi \leq s$. Also denote by $N(x)$ the set of neighboring cells of cell x. Then the set of all possible new paths are $P = \{\langle x_1^\varphi \rightarrow \cdots \rightarrow x_{t-1}^\varphi \rightarrow x \rangle | x \in N(x_l^\varphi) \bigcup \{x_l^\varphi\}, 1 \leq \varphi \leq s\}$. The CITS server then finds the s paths with the smallest overall path RSS difference and returns the last reference location of the most likely path as the user's current location.

In what follows, we detail the procedure of estimating the user's location at each time $t = 1, 2, \ldots$.

1) At Time $t = 1$: Since the user has submitted only one RSS measurement rss_1 at time $t = 1$ which is insufficient for path matching, we estimate the user's location l_1 according to the classical RSS-IPS Radar [8] and record the s most likely reference locations for later path matching.

Specifically, on receiving the user's RSS measurement $\mathsf{rss}_1 = (\mathsf{rss}_1^1, \ldots, \mathsf{rss}_1^m)$, we estimate the user's location at time 1 as

$$l_1 = \arg\min_{x \in V} \sum_{j=1}^{m} (\mathsf{rss}_x^j - \mathsf{rss}_1^j)^2 \ , \tag{6}$$

which is the reference location with the closest RSS fingerprint to rss_1 measured by the Euclidean distance. In addition, we also record the set of s reference locations whose RSS fingerprints are closest to rss_1, denoted by P_1.

2) At Time $t = 2$: On receiving the user's RSS measurement rss_2 at time $t = 2$, we estimate the user's location l_2 via path matching.

First, we generate a set of candidate paths from the set of most likely reference locations S_1 and graph G. Specifically, for each reference location $x \in P_1$, we generate a set of candidate path as $C_x = \{\langle x \rightarrow y \rangle | y \in N(x) \bigcup \{x\}\}$. The set of all candidate paths is then $C = \bigcup_{x \in P_1} C_x$.

Second, we find the candidate path with the smallest overall path difference whereby to determine the user's current location l_t. Specifically, for every candidate path $p = \langle x \rightarrow y \rangle \in P$, we computes its overall path difference as

$$\begin{aligned} \phi_{\langle x \rightarrow y \rangle} &= \phi(2, e(x, y)) \\ &= \sum_{j=1}^{m} |\triangle \mathsf{rss}_t^j - \triangle \mathsf{rss}_{x,y}^j| \ . \end{aligned} \tag{7}$$

The most likely path is then given by

$$\langle x^*, y^* \rangle = \arg\min_{\langle x \rightarrow y \rangle \in C} \phi_{\langle x \rightarrow y \rangle} \ ,$$

and the user's current location is estimated as $l_2 = y^*$. Moreover, we also record the set of s most likely paths denoted by P_2.

3) At Time $t > 2$: On receiving the user's RSS measurement rss_t at time $t > 2$, we estimate the user's location l_t in a similar fashion.

First, we generate a set of candidate paths from the set of most likely paths P_{t-1} and graph G. Specifically, for each path $p = \langle x_1 \rightarrow \cdots \rightarrow x_{t-1} \rangle \in P_{t-1}$, we generate a set of candidate path as $C_p = \{\langle x_1 \rightarrow \cdots \rightarrow x_{t-1} \rightarrow y \rangle | y \in N(x_{t-1}) \bigcup \{x_{t-1}\}\}$. The set of all candidate paths is then $C = \bigcup_{p \in P_{t-1}} C_p$.

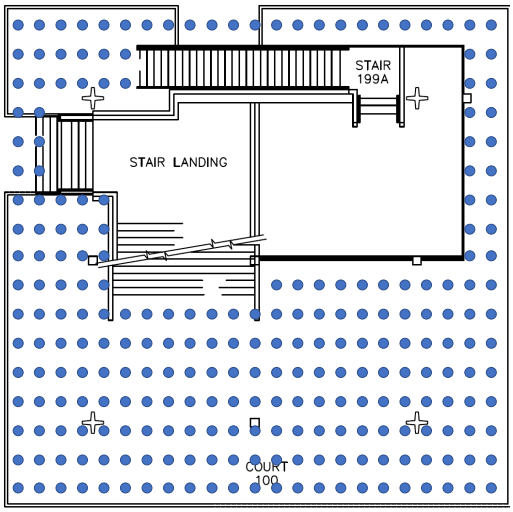

Fig. 2. The floor plan of the office space

Second, we find the candidate path with the smallest overall path difference whereby to determine the user's current location l_t. Specifically, for every candidate path $p = \langle x_1 \rightarrow \cdots \rightarrow x_{t-1} \rightarrow y \rangle \in C$, we computes its overall path difference as

$$\begin{aligned} \phi_p &= \phi_{\langle x_1 \rightarrow \cdots \rightarrow x_{t-1} \rightarrow y \rangle} \\ &= \sum_{i=1}^{t-1} \phi(i, e(x_{i-1}, x_i)) + \phi(t, e(x_{t-1}, y)) \ . \end{aligned}$$

The most likely path is then given by

$$\langle x_1^* \rightarrow \cdots \rightarrow x_t^* \rangle = \arg\min_{p \in C} \phi_p \ ,$$

and the user's current location is estimated as $l_t = x_t^*$. Moreover, we also record the set of s most likely paths denoted by P_t.

We summarize the whole procedure in Algorithm 1.

IV. Performance Evaluation

In this section, we evaluate the performance of CITS via detailed experimental studies based on real prototype.

A. Prototype Implementation and Data Collection

We implement a prototype of CITS in Android studio/Java and deploy it on a square zone of 23.8×23.8 m^2 inside an office building with the floor plan shown in Fig. 2. We chose $n = 368$ reference locations in the indoor venue and detected $m = 41$ WiFi APs based on unique SSIDs.

We use three models of smartphones for our data collection, including a Huawei Honor 8 (HH8), a Motorala One (MO), and a Google Pixel 6 (GP6). Table. II summarizes the configuration of each smartphone model. For each reference location,

Algorithm 1: Location Estimation

input : Graph $G = (V, E)$, RSS measurement rss_t at time $t = 1, 2, \ldots$, parameter s
output: User's location l_t at each time t

if $t = 1$ **then**
  $l_1 \leftarrow \arg\min_{x \in V} \sum_{j=1}^{m} (\mathsf{rss}_x^j - \mathsf{rss}_1^j)^2$;
  Record the set of s most likely reference locations as P_1;
end
if $t = 2$ **then**
  foreach $x \in P_1$ **do**
    $C_x \leftarrow \{\langle x \rightarrow y \rangle | y \in N(x) \bigcup \{x\}\}$;
  end
  $C \leftarrow \bigcup_{x \in P_1} C_x$;
  foreach $\langle x \rightarrow y \rangle \in C$ **do**
    $\phi_{\langle x \rightarrow y \rangle} \leftarrow \sum_{j=1}^{m} |\triangle \mathsf{rss}_t^j - \triangle \mathsf{rss}_{x,y}^j|$;
  end
  $\langle x^*, y^* \rangle \leftarrow \arg\min_{\langle x \rightarrow y \rangle \in C} \phi_{\langle x \rightarrow y \rangle}$;
  $l_2 \leftarrow y^*$;
  Record the set of s most likely candidate paths as P_2;
end
if $t > 2$ **then**
  foreach $p = \langle x_1 \rightarrow \cdots \rightarrow x_{t-1} \rangle \in P_{t-1}$ **do**
    $C_p \leftarrow \{\langle x_1 \rightarrow \cdots \rightarrow x_{t-1} \rightarrow y) | y \in N(x_{t-1}) \bigcup \{x_{t-1}\}\}$;
  end
  $C \leftarrow \bigcup_{p \in P_{t-1}} C_p$;
  foreach $p = \langle x_1 \rightarrow \cdots \rightarrow x_{t-1} \rightarrow y) \in C$ **do**
    $\phi_p \leftarrow \sum_{i=1}^{t-1} \phi(i, e(x_{i-1}, x_i)) + \phi(t, e(x_{t-1}, y))$;
  end
  $\langle x_1^* \rightarrow \cdots \rightarrow x_t^* \rangle \leftarrow \arg\min_{p \in C} \phi_p$;
  $l_t \leftarrow x_t^*$;
  Record the set of s most likely candidate paths as P_t;
end
return l_t;

we record its coordinate and collect RSS measurement using all three smartphones at the same time. We then create three differential RSS fingerprint databases with one for each smartphone.

We then use each of three smartphones to collect 60 movement traces. For each trace, we have one user carrying the smartphone walk in the indoor venue randomly for a duration of 28 seconds. The user stops every 1 second to record a test location and collects the corresponding RSS measurement. Note that the test locations may not be the same as any reference location.

Since CITS is mostly related to RADAR [54], the classical RSS-IPS that matches a user's RSS measurement to the reference location with the closest RSS fingerprint, we compare it with RADAR, i.e., the server estimates the user's location via RADAR on receiving the user's RSS measurement. Moreover, we use *error distance* as our performance metric, which is defined as the user's true location and the estimated reference location.

TABLE I
DEFAULT EXPERIMENT SETTINGS

Para.	Value	Description
n	368	# of reference locations
m	41	# of APs
	1.1 m	The size of each cell
	1 m	User's maximum travel distance
d	2.2 m	Maximum distance between two vertexes connected by an edge
s	15	# of candidate paths recorded

B. Experiment Results

We now report our experiment results.

1) Validation of Device Diversity: Since CITS relies on the assumption that there is a linear relationship between two devices' RSS measurements from the same AP at the same location and time and that the slope of the linear relationship is close to one, we first validate this assumption using the RSS measurements collected by different devices at the same location and time.

Figs. 3(a) to 3(c) plot the relationships between the RSS measurements collected by GP6 and MO, those collected by HH8 and MO, and those collected by GP6 and HH8, respectively. As we can see from all three figures, the RSS measurements collected by difference devices at the same locations and times exhibit a linear relationship, which is expected.

We further perform linear regression on RSS measurements collected by each pair of devices according to both Eq. (1) and Eq. (2). Tables III and IV show the parameters obtained from the two types of linear regression, respectively. As we can see from Table III, the slope of the linear equation under Eq. (1) ranges from 0.78 to 1.26 and the Mean Square Error (MSE) ranges from 0.74 to 0.94 for the six pairs of devices. In addition, Table IV shows that the MSE ranges from 1.19 to 1.94 if we set the slope to one according to Eq. (2). While the MSE achieved under Eq. (2) is larger than that under Eq. (1), these results do indicate that it is reasonable to assume that the slope is one. As we will see shortly, CITS works well in practice under this assumption.

2) Error Distance Over Time: Figs. 4(a) to 4(c) compare the average error distances of CITS and RADAR at each time with the user's RSS measurements collected by HH8, MO, and GP6, respectively, where the differential RSS fingerprint

TABLE II
SMARTPHONE CONFIGURATIONS

Brand	Model	CPU	RAM
Huawei	Honor 8	2.3GHz Octa-core	4G
Motorala	One	2GHz ARM Cortex-A53	4G
Google	Pixel 6	2.8GHz Octa-core	8G

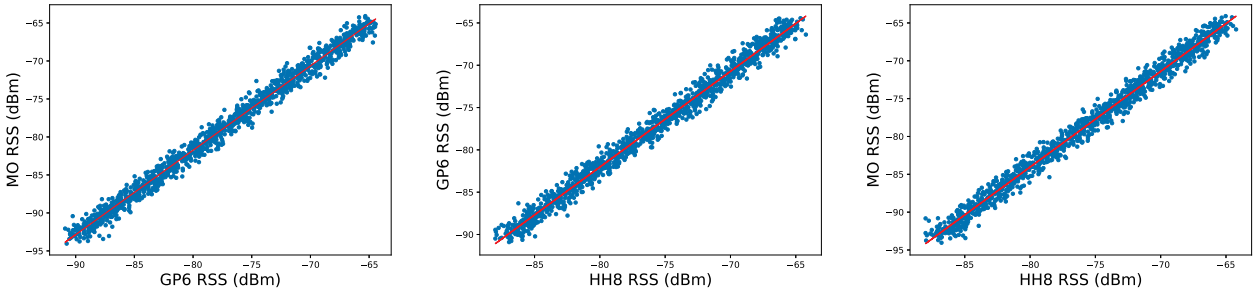

(a) GP6 vs. MO (b) HH8 vs. GP6 (c) HH8 vs. MO

Fig. 3. Relationship between RSS measurements collected by different pairs of devices

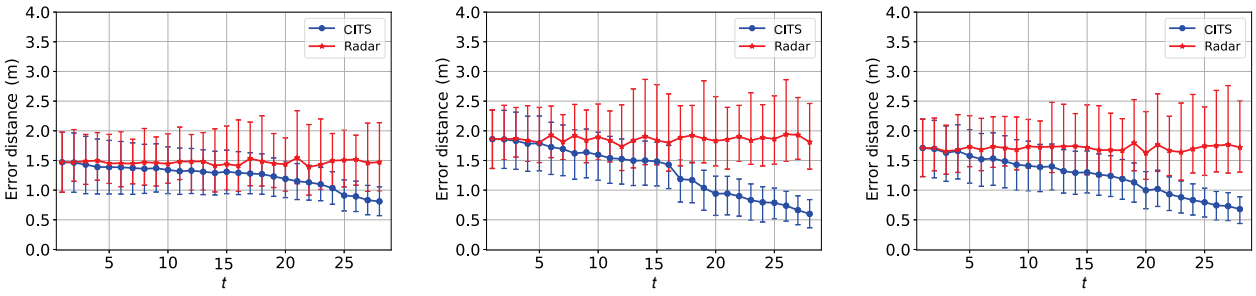

(a) Error distance vs. t (HH8) (b) Error distance vs. t (MO) (c) Error distance vs. t (GP6)

Fig. 4. Error distance with different user devices and differential RSS fingerprint database constructed from RSS measurements collected by HH8

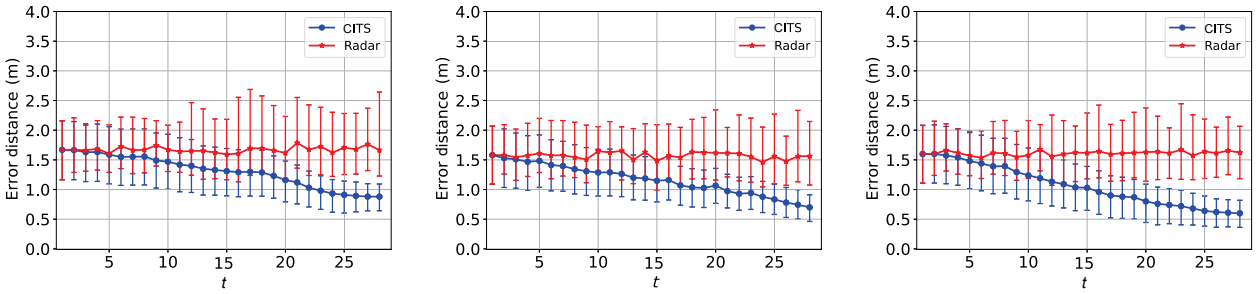

(a) Error distance vs. t (HH8) (b) Error distance vs. t (MO) (c) Error distance vs. t (GP6)

Fig. 5. Error distance with different user devices and differential RSS fingerprint database constructed from RSS measurements collected by MO

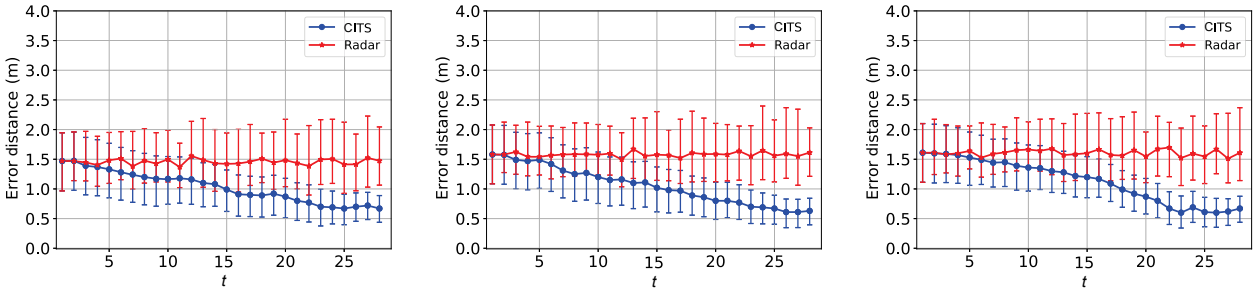

(a) Error distance vs. t (HH8) (b) Error distance vs. t (MO) (c) Error distance vs. t (GP6)

Fig. 6. Error distance with different user devices and differential RSS fingerprint database constructed from RSS measurements collected by GP6

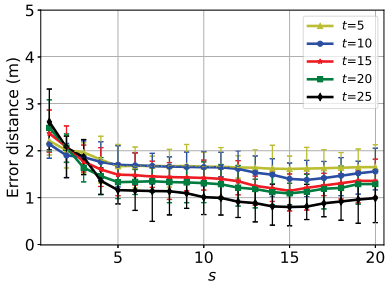

(a) Error distance vs. s

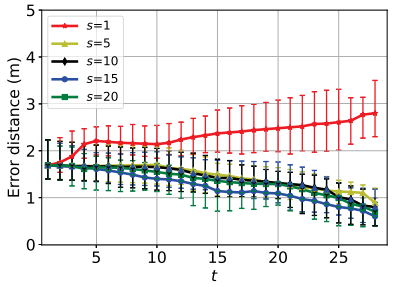

(b) Error distance vs. t

Fig. 7. The average distance error of CITS over time under different s.

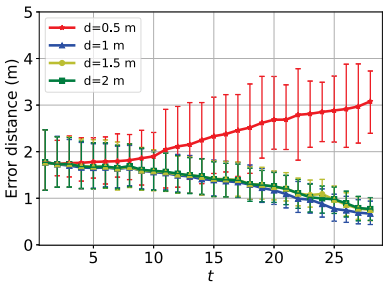

Fig. 8. The average distance error of CITS over time under different d.

TABLE III
LINEAR REGRESSION UNDER EQ. (1)

Device A	Device B	θ	δ_{AB}	MSE
GP6	MO	1.11	7.29	0.89
HH8	GP6	1.12	8.34	0.86
HH8	MO	1.26	17.21	0.94
GP6	HH8	0.87	-8.37	0.76
MO	HH8	0.78	-14.44	0.74
MO	GP6	0.88	-7.42	0.80

TABLE IV
LINEAR REGRESSION UNDER EQ. (2)

Device A	Device B	θ	δ_{AB}	MSE
GP6	MO	1	-1.48	1.21
HH8	GP6	1	-1.50	1.19
HH8	MO	1	-2.99	1.94
GP6	HH8	1	1.50	1.19
MO	HH8	1	2.99	1.94
MO	GP6	1	1.48	1.21

database is constructed from the RSS measurements collected by HH8 and every bar represents the 70% confidence interval.

We can see from Figs. 4(a) to 4(c) that the average error distance under RADAR is relatively stable across different times. This is expected, as RADAR treats every RSS measurement from the user as an independent location query and does not consider the user's past location. In addition, the average error distance under RADAR is 1.49 m, 1.88 m, and 1.75 m for HH8, MO, and GP6, respectively. Among them, the average error distance for HH8 is the lowest, which is anticipated because the differential RSS fingerprint database is constructed from the measurements collected by the same device. These results further confirm the negative impact of device diversity on positioning accuracy. In contrast, we can see from all three figures that the error distance of CITS matches that of RADAR at time $t = 1$ initially and decreases over time for all three different user devices. This is also anticipated, because CITS estimates the user's location at time $t = 1$ according to RADAR and thus has the same error distance as RADAR. In addition, CITS locates the user through differential RSS fingerprint matching and path matching at time $t \geq 2$ that can effectively mitigate the impact of device diversity and achieve higher positioning accuracy over time. For example, we can see from Fig. 4(b) that the average error distance decreases from 1.49 m at time $t = 1$ to 0.53 m at time $t = 28$.

Figs. 5 and 6 show the average error distances of CITS and RADAR at each time with the user's RSS measurements collected by HH8, MO, and GP6, respectively, where the differential RSS fingerprint database is constructed from the RSS measurements collected by MO and GP6, respectively. Similar to what we have seen from Fig. 4, the average error distance under RADAR is relatively stable across different times for all cases. Moreover, the average error distance is the lowest when the user's device is the same as the device used for collect RSS fingerprints. Last but not the least, the average error distance of CITS decreases over time. These results clearly demonstrate the advantages of CITS over Radar.

3) The Impact of Parameter s: Fig. 7 shows the average error distance of CITS at different times and under different s, i.e., the number of most likely candidate paths that the server records at every time. Specifically, Fig. 7 shows the average error distance of CITS at time $t = 5, 10, 15, 20$, and 25 as s increases from 1 to 20. We can see from Fig. 7(a) that the average error distance of CITS first decreases quickly as s increases from 1 to 5, then decreases relatively slowly as s further increases from increases from 5 to 15, and finally remains relatively stable or slightly fluctuates as s further increases from increases from 15 to 20. Consider $t = 25$ as an example. The average error distance decreases from 2.6 m to 0.80 m as s increases from 1 to 15, and then slightly increases to 0.99 m as s further increases to 20. The reason for the initial decrease in the average distance error is the more most likely candidate paths that the server stores, the higher possibility that the user's true path is among them. Therefore, the average error distance decreases initially. Moreover, having the server records too many most likely candidate paths at each time t could negatively affect positioning accuracy. The reason is there is non-negligible probability that a candidate paths ranked lowly earlier may become a top ranked path at some point due to the fluctuation of RSS and thus mislead the server into choosing an incorrect path. Therefore, parameter s needs to be carefully chosen. Our experiment results show that CITS achieves the best positioning accuracy when $s = 15$.

Fig. 7(b) shows the average error distance of CITS over

time for $s = 1, 5, 10, 15$, and 20. We can see that the average error distance of CITS increases over time when $s = 1$. This is expected, as the true path may not be the most likely path determined via path matching. Once an incorrect path is selected by the CITS server, subsequent location estimations will be affected by previous positioning error, which would result in increased error distance over time. Moreover, we can also see that the error distance of CITS decreases over time if s is larger than 5. This is expected and also confirms the effectiveness of the path matching.

4) The Impact of Parameter d: Recall that the differential RSS fingerprint database requires us to construct a graph $G = (V, E)$, in which any two vertexes are connected by an edge if the minimal distance between the two cells they represent is smaller than d. Ideally, parameter d should be set sufficiently large so that it is impossible for a user to travel from one cell to another cell that are not connected by any edge between two consecutive RSS measurements.

Fig. 8 shows the the average error distance of CITS over time with d varying from 0.5 m to 2 m where the true maximum travel distance of the user is 1 m. We can see that when $d = 0.5$ m that is smaller than the true true maximum travel distance of the user, the average error distance of CITS increases from 1.77 m at $t = 1$ to 3.08 m at time $t = 28$. This is expected because if d is set too small, the graph G does not contain the user's true path. As a result, CITS is unable to find the user's path and correctly estimate the user's location. Moreover, we can also see that when average error distance of CITS decreases over time for $d = 1$ m, 1.5 m, and 2 m. This is because d is sufficiently large and the user's true path can be captured and identified by CITS in these cases. Last but not the least, we can see that the average error distance of CITS at time $t > 25$ when $d = 2$ m is slightly larger than that when $d = 1$ m. This is also expected, because the larger d, the more candidate paths needs to be examined at each time, the higher the probability that an incorrect path is chosen by the CITS server, which would result in slightly higher error distance.

C. Summary

We summarize the experiment result as follows.

- Devices of different models could collect different RSS measurements at the same time and location, but there is a linear relationship between the RSS measurements collected by different devices. It is also reasonable to assume that the RSS measurements collected by different devices differ by a device-specific constant.
- CITS achieves higher positioning accuracy than RADAR in the presence of device diversity and the average error distance of CITS decreases over time.
- CITS achieves higher positioning accuracy when the user's smartphone is of the same model as the one used for collecting RSS fingerprints.
- Parameters s and d both need to set sufficiently large to ensure that the user's true path is always included in the candidate path set at each time.
- Setting parameters s and d too large have a negative impact on the positioning accuracy of CITS due to the introduction of too many candidate paths.

V. Conclusion

In this paper, we have introduced the design and evaluation of CITS, a novel continuous indoor tracking system. CITS achieves high positioning accuracy in the presence of RSS fingerprint ambiguity and device diversity through differential RSS fingerprinting and path matching. Detailed experiment studies based on real prototype implementation have confirmed the significant advantages of CITS over prior alternative solutions. As our future work, we plan to investigate extending CITS by removing the assumption of $\theta = 1$ by gradually estimating θ as more RSS measurements are received.

Acknowledgement

The authors would like to thank the anonymous reviewers for their constructive comments and helpful advice. This work was supported in part by the US National Science Foundation under grants CNS-1651954 (CAREER) and CNS-1933047.

References

[1] "Global indoor positioning and navigation system market industry trends and forecast to 2028," 2021. [Online]. Available: https://www.databridgemarketresearch.com/reports/global-indoor-positioning-and-navigation-system-market

[2] G. Ruipeng, T. Yang, Y. Fan, L. Guojie, B. Kaigui, W. Yizhou, W. Tao, and L. Xiaoming, "Sextant: Towards ubiquitous indoor localization service by photo-taking of the environment," *IEEE Transactions on Mobile Computing*, vol. 15, no. 2, pp. 460–474, 2016.

[3] M. Liu, J. Du, Q. Zhou, Z. Cao, and Y. Liu, "Eyeloc: Smartphone vision-enabled plug-n-play indoor localization in large shopping malls," *IEEE Internet of Things Journal*, vol. 8, no. 7, pp. 5585–5598, 2021.

[4] Y. Li, R. H. Kambhamettu, Y. Hu, and R. Zhang, "Impos: An image-based indoor positioning system," in *IEEE CCNC*, 2022, pp. 144–150.

[5] J. Guangyao, L. Xiaoyi, and P. MyongSoon, "An indoor localization mechanism using active RFID tag," in *IEEE SUTC'06*, vol. 1, 2006, pp. 4 pp.–.

[6] S. S. Saab and Z. S. Nakad, "A standalone rfid indoor positioning system using passive tags," *IEEE Transactions on Industrial Electronics*, vol. 58, no. 5, pp. 1961–1970, 2011.

[7] F. Seco and A. R. Jimnez, "Smartphone-based cooperative indoor localization with rfid technology," *Sensors*, vol. 18, no. 1, 2018.

[8] P. Bahl and V. N. Padmanabhan, "Radar: an in-building rf-based user location and tracking system," in *IEEE INFOCOM*, vol. 2, Tel Aviv, Israel, March 2000, pp. 775–784.

[9] M. Youssef and A. Agrawala, "The horus wlan location determination system," in *ACM MobiSys*, Seattle, WA, June 2005, pp. 205–218.

[10] T. Q. Wang, Y. A. Sekercioglu, A. Neild, and J. Armstrong, "Position accuracy of time-of-arrival based ranging using visible light with application in indoor localization systems," *Journal of Lightwave Technology*, vol. 31, no. 20, pp. 3302–3308, 2013.

[11] X. Guo, S. Shao, N. Ansari, and A. Khreishah, "Indoor localization using visible light via fusion of multiple classifiers," *IEEE Photonics Journal*, vol. 9, no. 6, pp. 1–16, 2017.

[12] S. Zhu and X. Zhang, "Enabling high-precision visible light localization in today's buildings," in *ACM MobiSys'17*, Niagara Falls, NY, 2017, p. 96108.

[13] G. Fischer, B. Dietrich, and F. Winkler, "Bluetooth indoor localization system," 01 2004.

[14] Y. Wang, Q. Ye, J. Cheng, and L. Wang, "Rssi-based bluetooth indoor localization," in *IEEE MSN*, 2015, pp. 165–171.

[15] L. Kanaris, A. Kokkinis, A. Liotta, and S. Stavrou, "Fusing bluetooth beacon data with wi-fi radiomaps for improved indoor localization," *Sensors*, vol. 17, 2017.

[16] S. P. Tarzia, P. A. Dinda, R. P. Dick, and G. Memik, "Indoor localization without infrastructure using the acoustic background spectrum," in *Proceedings of MobiSys'11*, 2011, p. 155168.

[17] W. Huang, Y. Xiong, X.-Y. Li, H. Lin, X. Mao, P. Yang, Y. Liu, and X. Wang, "Swadloon: Direction finding and indoor localization using acoustic signal by shaking smartphones," *IEEE Transactions on Mobile Computing*, vol. 14, no. 10, pp. 2145–2157, 2015.

[18] H. Liu, Y. Gan, J. Yang, S. Sidhom, Y. Wang, Y. Chen, and F. Ye, "Push the limit of wifi based localization for smartphones," in *Proceedings of Mobicom'12*, 2012, pp. 305316.

[19] L. Yuan, Y. Hu, Y. Li, R. Zhang, Y. Zhang, and T. Hedgpeth, "Secure rss-fingerprint-based indoor positioning: Attacks and countermeasures," in *IEEE CNS'18*, Beijing, May 2018, pp. 1–9.

[20] S. Yang, P. Dessai, M. Verma, and M. Gerla, "FreeLoc: Calibration-free crowdsourced indoor localization," in *IEEE INFOCOM'13*, April 2013, pp. 2481–2489.

[21] F. Dong, Y. Chen, J. Liu, Q. Ning, and S. Piao, "A calibration-free localization solution for handling signal strength variance," *Mobile Entity Localization and Tracking in GPS-less Environnments*, vol. 5801, pp. 79–90, 2009.

[22] A. Goswami, L. E. Ortiz, and S. R. Das, "WiGEM: a learning-based approach for indoor localization," in *ACM CoNEXT '11*, Tokyo, Japan, 2011, pp. 3:1–3:12.

[23] J. geun Park, D. Curtis, S. Teller, and J. Ledlie, "Implications of device diversity for organic localization," in *IEEE INFOCOM'11*, April 2011, pp. 3182–3190.

[24] "Dead reckoning," 2021. [Online]. Available: https://en.wikipedia.org/wiki/Deadreckoning

[25] F. Lei, P. Antsaklis, L. Montestruque, M. McMickell, M. Lemmon, S. Yashan, F. Hui, I. Koutroulis, M. Haenggi, X. Min, and X. Xiaojuan, "Design of a wireless assisted pedestrian dead reckoning system - the navmote experience," *IEEE Transactions on Instrumentation and Measurement*, vol. 54, no. 6, pp. 2342–2358, 2005.

[26] C. Fischer, K. Muthukrishnan, M. Hazas, and H. Gellersen, "Ultrasound-aided pedestrian dead reckoning for indoor navigation," in *ACM MobiCom'08*, San Francisco, CA, Sept. 2008.

[27] S. House, S. Connell, I. Milligan, D. Austin, T. L. Hayes, and P. Chiang, "Indoor localization using pedestrian dead reckoning updated with rfid-based fiducials," in *2011 Annual International Conference of the IEEE Engineering in Medicine and Biology Society*, 2011, pp. 7598–7601.

[28] V. Radu and M. K. Marina, "Himloc: Indoor smartphone localization via activity aware pedestrian dead reckoning with selective crowdsourced wifi fingerprinting," in *International Conference on Indoor Positioning and Indoor Navigation*, 2013, pp. 1–10.

[29] P. Alexey, G. Andrey, and S. Alexey, "Indoor positioning using wi-fi fingerprinting pedestrian dead reckoning and aided ins," in *International Symposium on Inertial Sensors and Systems (ISISS'14)*, 2014, pp. 1–2.

[30] G. Lu, Y. Yan, L. Ren, P. Saponaro, N. Sebe, and C. Kambhamettu, "Where am i in the dark:exploring active transfer learning on the use of indoor localization based on thermal imaging," *Neurocomputing*, vol. 173, no. P1, p. 8392, jan 2016.

[31] L. Lin Shen and W. Wong Shung Hui, "Improved pedestrian dead-reckoning-based indoor positioning by rssi-based heading correction," *IEEE Sensors Journal*, vol. 16, no. 21, pp. 7762–7773, 2016.

[32] N.-H. Ho, P. H. Truong, and G.-M. Jeong, "Step-detection and adaptive step-length estimation for pedestrian dead-reckoning at various walking speeds using a smartphone," *Sensors*, vol. 16, no. 9, 2016.

[33] R. Ban, K. Kaji, K. Hiroi, and N. Kawaguchi, "Indoor positioning method integrating pedestrian dead reckoning with magnetic field and wifi fingerprints," in *Eighth International Conference on Mobile Computing and Ubiquitous Networking (ICMU)'15*, 2015, pp. 167–172.

[34] L. You, Z. Yuan, L. Haiyu, Z. Qifan, N. Xiaoji, and E.-S. Naser, "A hybrid wifi/magnetic matching/pdr approach for indoor navigation with smartphone sensors," *IEEE Communications Letters*, vol. 20, 2016.

[35] J. Kuang, X. Niu, P. Zhang, and X. Chen, "Indoor positioning based on pedestrian dead reckoning and magnetic field matching for smartphones," *Sensors*, vol. 18, no. 12, 2018.

[36] J. Yang and Y. Chen, "A theoretical analysis of wireless localization using rf-based fingerprint matching," in *2008 IEEE International Symposium on Parallel and Distributed Processing*, 2008, pp. 1–6.

[37] M. Hoang, J. Schmalenstroeer, C. Drueke, D. Tran Vu, and R. Haeb-Umbach, "A hidden markov model for indoor user tracking based on wifi fingerprinting and step detection," in *21st European Signal Processing Conference (EUSIPCO 2013)*, 2013, pp. 1–5.

[38] A. W. S. Au, C. Feng, S. Valaee, S. Reyes, S. Sorour, S. N. Markowitz, D. Gold, K. Gordon, and M. Eizenman, "Indoor tracking and navigation using received signal strength and compressive sensing on a mobile device," *IEEE Transactions on Mobile Computing*, vol. 12, no. 10, pp. 2050–2062, Oct 2013.

[39] H. Liu, N. Xia, D. Guo, and P. Qing, "Csi-based indoor tracking with positioning-assisted," in *Ubiquitous Positioning, Indoor Navigation and Location-Based Services (UPINLBS)'18*, 2018, pp. 1–8.

[40] Y. Wang, J. Liu, Y. Chen, M. Gruteser, J. Yang, and H. Liu, "E-eyes: Device-free location-oriented activity identification using fine-grained wifi signatures," in *Proceedings of the 20th Annual International Conference on Mobile Computing and Networking*, ser. MobiCom '14. New York, NY, USA: Association for Computing Machinery, 2014, p. 617628.

[41] K. Kleisouris, Y. Chen, J. Yang, and R. P. Martin, "The impact of using multiple antennas on wireless localization," in *2008 5th Annual IEEE Communications Society Conference on Sensor, Mesh and Ad Hoc Communications and Networks*, 2008, pp. 55–63.

[42] X. Zheng, H. Liu, J. Yang, Y. Chen, R. P. Martin, and X. Li, "A study of localization accuracy using multiple frequencies and powers," *IEEE Transactions on Parallel and Distributed Systems*, vol. 25, no. 8, pp. 1955–1965, 2014.

[43] Y. Shu, Y. Huang, J. Zhang, P. Cou, P. Cheng, J. Chen, and K. G. Shin, "Gradient-based fingerprinting for indoor localization and tracking," *IEEE Transactions on Industrial Electronics*, vol. 63, no. 4, pp. 2424–2433, 2016.

[44] H. Liu, J. Yang, S. Sidhom, Y. Wang, Y. Chen, and F. Ye, "Accurate wifi based localization for smartphones using peer assistance," *IEEE Transactions on Mobile Computing*, vol. 13, no. 10, pp. 2199–2214, 2014.

[45] J. Yang and Y. Chen, "Indoor localization using improved rss-based lateration methods," in *GLOBECOM 2009 - 2009 IEEE Global Telecommunications Conference*, 2009, pp. 1–6.

[46] N. Hernndez, M. Ocaa, J. M. Alonso, and E. Kim, "Wifi-based indoor localization and tracking of a moving device," in *2014 Ubiquitous Positioning Indoor Navigation and Location Based Service (UPINLBS)*, 2014, pp. 281–289.

[47] G. Chandrasekaran, M. A. Ergin, J. Yang, S. Liu, Y. Chen, M. Gruteser, and R. P. Martin, "Empirical evaluation of the limits on localization using signal strength," in *2009 6th Annual IEEE Communications Society Conference on Sensor, Mesh and Ad Hoc Communications and Networks*, 2009, pp. 1–9.

[48] I. Mai, T. Marwan, and E. Mustafa, "Cnn based indoor localization using rss time-series," in *IEEE Symposium on Computers and Communications (ISCC'18)*, 2018.

[49] P. Tiwary, A. Pandey, S. Kumar, and M. Youssef, "Novel differential r-vectors for localization in iot networks," *IEEE Sensors Letters*, vol. 5, no. 6, pp. 1–4, 2021.

[50] J. Yang, Y. Chen, V. B. Lawrence, and V. Swaminathan, "Robust wireless localization to attacks on access points," in *2009 IEEE Sarnoff Symposium*, 2009, pp. 1–5.

[51] X. Li, Y. Chen, J. Yang, and X. Zheng, "Designing localization algorithms robust to signal strength attacks," in *2011 Proceedings IEEE INFOCOM*, 2011, pp. 341–345.

[52] Y. Li, Y. Hu, R. Zhang, Y. Zhang, and T. Hedgpeth, "Secure indoor positioning against signal strength attacks via optimized multi-voting," in *2019 IEEE/ACM 27th International Symposium on Quality of Service (IWQoS)*, 2019, pp. 1–10.

[53] L. Li, G. Shen, C. Zhao, T. Moscibroda, J.-H. Lin, and F. Zhao, "Experiencing and handling the diversity in data density and environmental locality in an indoor positioning service," in *MobiCom'14*, Maui, Hawaii, USA, 2014, pp. 459–470.

[54] P. Bahl, V. N. Padmanabhan, and A. Balachandran, "Enhancements to the radar user location and tracking system," *Microsoft Research*, vol. 2, no. MSR-TR-2000-12, pp. 775–784, Feb. 2000.